Stability Analysis for Multiple Voltage Source Converters Connected at a Bus

Arindam Ghosh, Gerard Ledwich and Firuz Zare
School of Engineering System
Queensland University of Technology
Brisbane, Australia
a.ghosh@qut.edu.au, g.ledwich@qut.edu.au and
f.zare@qut.edu.au

Ritwik Majumder
Power Technology Group
ABB Corporate Research
Vasteras, Sweden
ritwik.majumder@se.abb.com

Abstract— This paper develops a tool for the stability analysis when multiple voltage controlled converters are connected to a distribution bus. In particular, the analysis is applicable to voltage source converters (VSCs) and has been extended to consider current control as well as voltage control. It is assumed that each VSC is controlled by a state feedback linear quadratic regulator (LQR) based switching design. A suitable model of the converter is first developed by including the state feedback gains. The model is then extended to incorporate parallel operation of two VSCs, connected to a bus. To consider autonomous operation, the power sharing arrangements without any explicit communication, i.e., droop controllers are incorporated in the model. Finally, a linearized model of the system is developed for Eigen analysis. It has been shown that the system response predicted by the developed model matches PSCAD simulation results very closely, thus confirming that the model developed can be used as an analytical tool.

Keywords- Voltage source converters, autonomous operation, linear quadratic control, stability analysis.

I. INTRODUCTION

In the past few decades, the use of power converters has become more common in uninterrupted power supply (UPS) application as well as in interfacing the micro sources in a distributed generation (DG) system. In a UPS application, the parallel operation of the converters can provide solution to improve capability, reliability and redundancy. In a distributed generation system, the micro sources, especially the intermittent types (like wind and solar), are interfaced through voltage source converters (VSCs) to the network [1].The converter can be used to maximize the energy yield from the micro source, control of output power and to improve power quality. The parallel connected converters control the power flow and quality by controlling the power conversion between the dc bus and the available grid [2].

Current regulator instability in parallel VSCs has been discussed in [3], in which a simple method of paralleling structures with carrier-based PWM current regulators to independently regulate each inverter's current is employed. The instability between the parallel inverters and the common motor can result in large uncontrolled currents, when the current regulators enter PWM over modulation region, resulting in a loss of current control.

However a current/load sharing mechanism has to be employed to avoid the overloading of any converters, especially when multiple converters are operating in an autonomous mode. Control of output power using output feedback is commonly used. Since the output currents of the converters are regulated at every switching instant, even with the harmonics in the output current, converters can share the current as desired.

The load sharing or the real and reactive power sharing can be achieved by controlling two independent quantities – frequency and the fundamental voltage magnitude [4, 5]. In [4], a control method for a converter feeding real and reactive power into a stiff system with a defined voltage is proposed, while [5] proposes a control scheme to improve the system transient stability. Both the paper uses frequency droop characteristics. In this paper however an angle droop is used as the power sharing mechanism [6].

A multi-converter system with instantaneous power sharing control is effectively a high order multi variable system. The VSCs should be controlled in such a manner that ensures a stable operation of the system. The system stability during load sharing has been further explored in [7-10]. Transient stability of a power system with high penetration level of power electronics interfaced (converter connected) distributed generation is explored in [7]. In [8], small-signal stability analysis of the combined droop and average power method for load sharing control of multiple distributed generation systems (DGs) in a stand-alone ac supply mode is discussed. The overall dynamics of the regulated converter is described in [9], where the characterization of regulated converters is addressed to enable the assessment of the stability, performance, supply and load interactions as well as transient responses. The stability analysis in autonomous operation is shown in [10]

 ISBN: 978-1-61208-136-6

in a hybrid system, where a wind-PV-battery system is feeding an isolated single-phase load.

In this paper, a model of a VSC that is operating in a closed-loop state feedback control is developed. The model is then extended to incorporate parallel operation of two VSCs. To consider autonomous operation, the power sharing arrangements through droop controllers, are incorporated in the model. Finally a linearized model of the system is developed for eigen analysis. Eigenvalues studies are performed with the mathematical expressions of the model using MATLAB. Also, all the results are verified through simulation studies using PSCAD. It is shown that the system response predicted by the model developed matches the PSCAD simulation results very closely.

A converter with its associate control affects the stability of a system that includes multiple VSCs. The main contribution of this paper is to demonstrate how the stability of such a system can be analyzed. This can be used as a screening tool before installing multiple parallel connected VSCs and choosing droop control parameters.

II. CONVERTER STRUCTURE AND CONTROL

All the DGs are assumed to consist of ideal dc voltage source supplying a voltage of V_{dc} to a VSC. The structure of the VSC is shown in Fig. 1. The VSC contains three H-bridges that are supplied from the common dc bus. The outputs of the H-bridges are connected to three single-phase transformers that are connected in wye for required isolation and voltage boosting [11]. The resistance R_T represents the switching and transformer losses, while the inductance L_T represents the leakage reactance of the transformers. The filter capacitor C_f is connected to the output of the transformers to bypass switching harmonics, while L_f represents an added output inductance of the DG system. Together L_T, C_f and L_f form an LCL or T-filter.

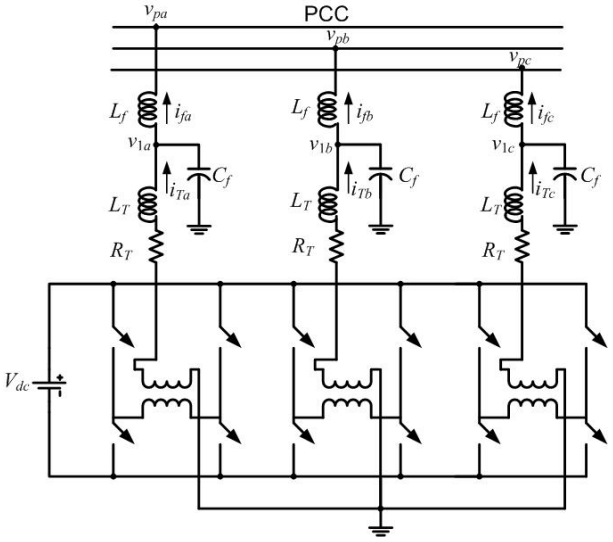

Figure 1. Converter structure.

The equivalent circuit of one phase of the converter is shown in Fig. 2. In this, $u \cdot V_{dc}$ represents the converter output voltage, where u is the switching function and is given by $u = \pm 1$. The main aim of the converter control is to generate u. From the circuit of Fig. 2, the following state vector is chosen

$$z^T = \begin{bmatrix} i_T & i_f & v_c \end{bmatrix} \tag{1}$$

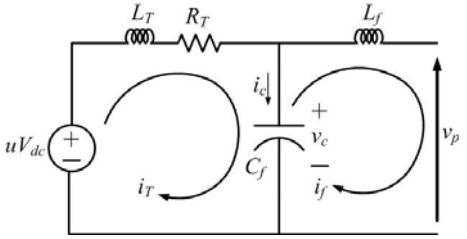

Figure 2. Single-phase equivalent circuit of VSC.

Then the state space equation of the system can be written as

$$\dot{z} = Az + Bu_c + Cv_p \tag{2}$$

where u_c is the continuous time approximation of the switching function u. and

$$A = \begin{bmatrix} -R_T/L_T & 0 & -1/L_T \\ 0 & 0 & 1/L_f \\ 1/C_f & -1/C_f & 0 \end{bmatrix}, B = \begin{bmatrix} V_{dc}/L_T \\ 0 \\ 0 \end{bmatrix}, C = \begin{bmatrix} 0 \\ -1/L_f \\ 0 \end{bmatrix}$$

The main aim of the converter control is to generate u_c from a suitable state feedback control law such that the output voltage and current are tracked properly according to their references. It is easy to generate references for the output voltage v_c and current i_f from power flow condition. However, the same cannot be said about the reference for the current i_T. On the other hand, once the reference for v_c is obtained, it is easy to calculate a reference for the current i_c through the filter capacitor (see Fig. 2).

To facilitate this, we define a new set of state vectors as

$$x^T = \begin{bmatrix} i_c & i_f & v_c \end{bmatrix} \tag{3}$$

We then have the following state transformation matrix

$$x = \begin{bmatrix} 1 & -1 & 0 \\ 0 & 1 & 0 \\ 0 & 0 & 1 \end{bmatrix} z = C_P z \tag{4}$$

The transformed state space equation is then given by combining (2) and (4) as

$$\dot{x} = C_p A C_p^{-1} x + C_p B u_c + C_p C v_p \tag{5}$$

If the system of (5) is sampled with a sampling time of ΔT, then its discrete-time description can be written in the form

$$x(k+1) = Fx(k) + Gu_c(k) + Hv_p(k) \tag{6}$$

To control the converter, we shall employ a discrete time line quadratic regulator which has the form

$$\begin{aligned} u_c(k) &= -K\left[x(k) - x_{ref}(k)\right] \\ &= \begin{bmatrix} k_1 & k_2 & k_3 \end{bmatrix}\left[x_{ref}(k) - x(k)\right] \\ &= k_1\left(i_{cref} - i_c\right) + k_2\left(i_{fref} - i_f\right) + k_3\left(v_{cref} - v_c\right) \end{aligned} \tag{7}$$

where x_{ref} is the reference vector and K is the feedback gain matrix obtained using discrete time linear quadratic regulator (LQR) with a state weighting matrix of Q and a control penalty of r. From $u_c(k)$, the switching function is generated as

$$\begin{aligned} &\text{If } u_c(k) > h \text{ then } u = +1 \\ &\text{elseif } u_c(k) < -h \text{ then } u = -1 \end{aligned} \tag{8}$$

where h is a small number. We shall now demonstrate the effectiveness of the control through the following example.

A Linear Quadratic Regulator is shown to produce an infinite gain margin and a phase margin of at least 60° [12]. Another important aspect of the LQR is that it is tolerant of input nonlinearities. The LQR design is stable provided that the effective gain of the input nonlinearity is constrained in the sector between ½ and 2 [12]. When the errors are large, and the control is bounded between + 1 and – 1 the elements of the gain matrix K must be small. For a set of decreasing values of r, we get a corresponding set of increasing values of K. Thus there always exists a value of r such that Kx is bounded appropriately. If we start from a finite set of state errors, there will be a K such that $K(x - x_{ref})$ will satisfy the upper sector bound, and since the system is open loop stable, the lower bound is not essential.

Example 1: In this example, let us assume that the VSC of Fig. 1 is connected to an infinite bus at the PCC. The system parameters considered for the study are given in Table I. To design the discrete-time controller, we have chosen a diagonal state weighting matrix as Q = diag(1 1000 10) and the control weighting as 0.01. This choice of Q emphasizes a maximum tracking effort on i_f and a minimum on i_c. The sampling time is chosen as 10 μs. The resultant gain matrix is K = [0.4338 8.3977 0.8405].

The desired converter output voltage is 11 kV (L-L, rms) with a phase angle of 30° (which translates into an instantaneous phase voltage of 8.98 kV peak). This sets the references of the currents from simple circuit laws. The peak of i_f reference is 59.195 A with an angle of 15°, while the peak of i_c reference is $\omega C_f 9.98\times10^3$ A and its phase angle 60°, i.e., leading v_c by 30°. The nine instantaneous reference quantities (3 for each phase are formed) and are tracked using the control law given in (7) and (8).

TABLE I. : SYSTEM PARAMETERS FOR EXAMPLE 1.

System Quantities	Values
Systems frequency	50 Hz
PCC voltage V_p	11 kV (L-L, rms)
PCC voltage phase	0° (Reference)
DC voltage V_{dc}	3.0 kV
Single-phase transformers	3//11 kV, with 10% leakage reactance (L_T = 31.8 mH)
Transformer losses R_T	0.1 Ω
Filter capacitor C_f	50 μF
Filter inductance L_f	250 mH

The results are shown in Fig. 3. The converter output voltages and the injected currents (i_f) and their references (dotted lines) are shown in this figure. It can be seen that the transients die out within 2½ cycles (0.05 s) and the converter tracks the reference quantities.

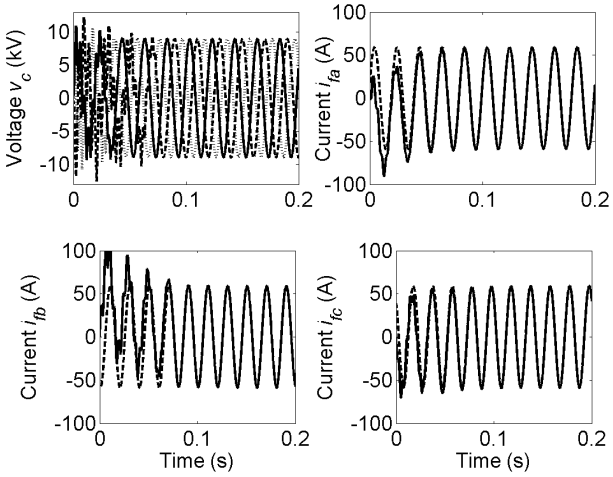

Figure 3. Voltage and current tracking in Example 1.

III. MATHEMATICAL MODEL OF VSC

In this section, a composite model of the converter in the d-q domain is developed, which includes the controller as well. Traditional sliding mode design consider a function S and control such that $S\dot{S} \le 0$. Then the system will approach $S = 0$, which is called the sliding line [13, 14]. When a finite switch rate constraint is applied, the system will chatter around $S = 0$, at the switching frequency. For switching at ± 1, the magnitudes of the switch frequency terms are all less than 1. When the system gain, at switch frequency and above, is less than α, then the system response at switch frequency is less than α. Thus when the system has sufficient lowpass filtering, its dynamics will follow the switching line with a negligible error. Since the VSC has an LCL filter to bypass the switch frequency harmonics, we can model the

system as if it is on the sliding line. It is however to be noted that this model reduction will fail if there is a system resonance near the switch frequency. Therefore the choice of the filter parameters is critical.

A. Converter Model

From equivalent circuit shown in Fig. 2, the following equations are obtained for each of the phases of the three-phase system

$$\frac{di_T}{dt} = -\frac{R_T}{L_T} i_T + \frac{\left(-v_c + u_c.V_{dc}\right)}{L_T} \tag{9}$$

$$\frac{dv_c}{dt} = \frac{\left(i_T - i_f\right)}{C_f} \tag{10}$$

$$v_c - v_p = L_f \frac{di_f}{dt} \tag{11}$$

Equations (9-11) are transformed into a *d-q* reference frame of converter output voltages, rotating at system frequency ω, where *a-b-c* to *d-q* transformation matrix P is given by

$$P = \frac{2}{3}\begin{bmatrix} \cos(\omega t) & \cos\left(\omega t - \frac{2\pi}{3}\right) & \cos\left(\omega t + \frac{2\pi}{3}\right) \\ -\sin(\omega t) & -\sin\left(\omega t - \frac{2\pi}{3}\right) & -\sin\left(\omega t + \frac{2\pi}{3}\right) \\ \frac{1}{2} & \frac{1}{2} & \frac{1}{2} \end{bmatrix}$$

Defining a state vector as

$$x_i = [i_{Td} \quad i_{Tq} \quad i_{fd} \quad i_{fq} \quad v_{cd} \quad v_{cq}]^T \tag{13}$$

the state equation in the *d-q* frame is given by

$$\dot{x}_i = A_i x_i + B_i u_{cdq} + C_i v_{pdq} \tag{14}$$

where u_{cdq} and v_{tdq} are two vectors containing the d and q axis components of u_c and v_t and

$$A_i = \begin{bmatrix} -R_T/L_T & \omega & 0 & 0 & -1/L_T & 0 \\ -\omega & -R_T/L_T & 0 & 0 & 0 & -1/L_T \\ 0 & 0 & 0 & \omega & 1/L_f & 0 \\ 0 & 0 & -\omega & 0 & 0 & 1/L_f \\ 1/C_f & 0 & -1/C_f & 0 & 0 & \omega \\ 0 & 1/C_f & 0 & -1/C_f & -\omega & 0 \end{bmatrix}$$

$$B_i = \begin{bmatrix} V_{dc}/L_T & 0 \\ 0 & V_{dc}/L_T \\ 0 & 0 \\ 0 & 0 \\ 0 & 0 \\ 0 & \end{bmatrix} \quad \text{and} \quad C_i = \begin{bmatrix} 0 & 0 \\ 0 & 0 \\ -1/L_f & 0 \\ 0 & -1/L_f \\ 0 & 0 \\ 0 & 0 \end{bmatrix}$$

From (7) and (4), u_c can be expressed as

$$u_c = k_1\left(i_{cref} - i_T + i_f\right) + k_2\left(i_{fref} - i_f\right) + k_3\left(v_{cref} - v_c\right)$$

The above equation can be expressed as

$$u_c = -k_1 i_T + \left(k_1 - k_2\right) i_f - k_3 v_c + k_1 i_{cref} + k_2 i_{fref} + k_3 v_{cref} \tag{15}$$

From (15), the d and q components of u_c are given as

$$\begin{bmatrix} u_d \\ u_q \end{bmatrix} = G_i x_i + H_i x_{refdq} \tag{16}$$

where

$$G_i = \begin{bmatrix} -k_1 & 0 & \left(k_1 - k_2\right) & 0 & -k_3 & 0 \\ 0 & -k_1 & 0 & \left(k_1 - k_2\right) & 0 & -k_3 \end{bmatrix}$$

$$H_i = \begin{bmatrix} k_1 & 0 & k_2 & 0 & k_3 & 0 \\ 0 & k_1 & 0 & k_2 & 0 & k_3 \end{bmatrix}$$

$$x_{refdq} = [i_{cdref} \quad i_{cqref} \quad i_{fdref} \quad i_{fqref} \quad v_{cdref} \quad v_{cqref}]^T$$

Substituting (16) into (14) we get

$$\dot{x}_i = \left(A_i + B_i G_i\right) x_i + B_i H_i x_{refdq} + C_i v_{pdq} \tag{17}$$

B. Computation of References

To solve the state equation (17), the reference vector x_{refdq} is required as input. In this sub-section, we shall discuss how they can easily be written in terms of the known quantities. We must however remember that all the d-q quantities are expressed in the reference frame of the converter output

voltages. Let us define the three-phase instantaneous reference converter output voltages as

$$v_{caref} = V_{cm}\sin(\omega t), \quad v_{cbref} = V_{cm}\sin(\omega t - 120°),$$
$$v_{ccref} = V_{cm}\sin(\omega t + 120°)$$

Then the transformation (19) will result in

$$\begin{bmatrix} v_{cdref} \\ v_{cqref} \end{bmatrix} = \begin{bmatrix} 0 \\ -V_{cm} \end{bmatrix} \tag{18}$$

Consequently, the reference for the capacitor currents that are leading the corresponding voltages by 90° are given as

$$\begin{bmatrix} i_{cdref} \\ i_{cqref} \end{bmatrix} = \begin{bmatrix} V_{cm}\omega C_f \\ 0 \end{bmatrix} \tag{19}$$

Now the expression for the power and reactive power are given by

$$P = \frac{3}{2}\left(v_d i_d + v_q i_q\right) \tag{20}$$

$$Q = \frac{3}{2}\left(v_q i_d - v_d i_q\right) \tag{21}$$

Let the real and reactive power that are desired to be injected to the PCC by the converter be denoted respectively P_{ref} and Q_{ref}. Then from (18), (20) and (21) we can write

$$\begin{bmatrix} i_{fdref} \\ i_{fqref} \end{bmatrix} = -\frac{2}{3V_{cm}}\begin{bmatrix} Q_{ref} \\ P_{ref} \end{bmatrix} \tag{22}$$

Combining (18), (19) and (22) we form the reference vectors in terms of V_{cm}, P_{ref} and Q_{ref}.

C. Transformation into a Common Reference Frame

The reference quantities are defined in terms of the reference frame of the converter output voltage. These need to be converted into a common reference frame. Let us choose the PCC voltage as the reference frame D-Q. Let also the angle between the PCC voltage and the converter voltage be δ. Then the relation between these two frames is shown in Fig. 4. From these figure we can write

$$\begin{bmatrix} f_D \\ f_Q \end{bmatrix} = \begin{bmatrix} \cos\delta & -\sin\delta \\ \sin\delta & \cos\delta \end{bmatrix}\begin{bmatrix} f_d \\ f_q \end{bmatrix} = T\begin{bmatrix} f_d \\ f_q \end{bmatrix} \tag{23}$$

All the reference d-q quantities are pre-multiplied by T to transform them in D-Q frame. The converter equation (17) can then be re-written as

$$\dot{x}_i = \left(A_i + B_i G_i\right)x_i + B_i H_i x_{refDQ} + C_i v_{pDQ} \tag{24}$$

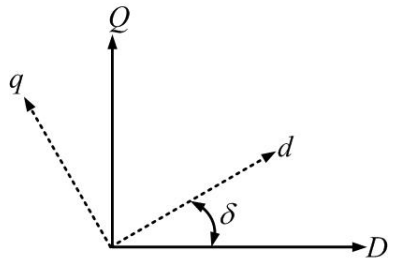

Figure 4. Relation between d-q and D-Q frames.

Example 2: In this example, we shall investigate the converter model developed in (24) and compare the results obtained with those of Example 1. Therefore the system parameters that are chosen are the same as those given in Example 1. For this case, the real and reactive power injected by the converter are 770.3 kW and 206.4 kVAr respectively. The state equations are solved in MATLAB. The three-phase converter output voltage and injected current are shown in Fig. 5. It can be seen that the steady state response of these quantities are almost identical to those of Fig. 3.

Comparing the responses in Figs. 3 and 5, it can be seen that they differ in the initial starting period. During this period, the system is trying to reach the sliding line. Once the system is on this line, the two responses are nearly identical. This is illustrated in this above example. Once the system is on the sliding line, it is robust to perturbations to system operating conditions, as will be illustrated in some of the subsequent examples. Therefore the model presented can be used for eigenvalue analysis and system response prediction

IV. Mathematical Model of Two VSCs Operating in Parallel

In this section, we develop the model when two VSCs are operating in parallel. The single-line diagram of the system considered is shown in Fig. 6. In this, the PCC is connected to an infinite bus with a voltage of v_s. A load, with an impedance of $R_L + j\omega L_L$ is connected to the PCC. The load current is denoted by i_L. The system parameters and quantities of the two VSCs are denoted by subscripts 1 and 2.

 ISBN: 978-1-61208-136-6

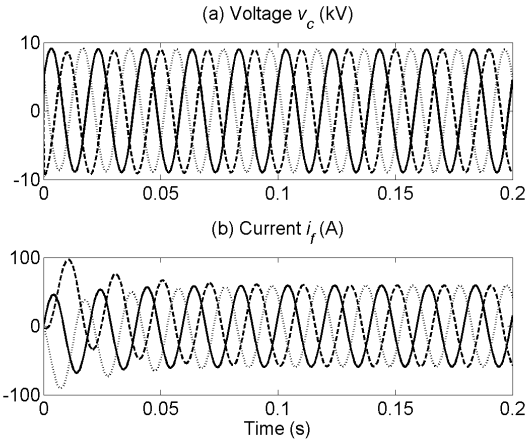

Figure 5. Output voltage and injected current for Example 2.

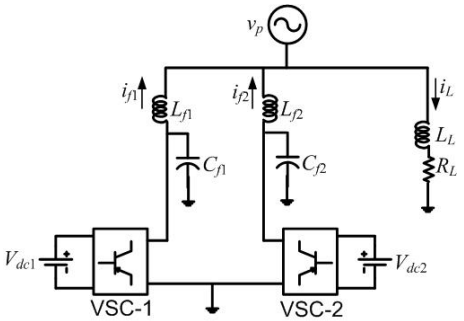

Figure 6. Single-line diagram of parallel operation of two VSCs.

The state equations of the VSCs can be written in the form (24) as

$$\dot{x}_{i1} = \left(A_{i1} + B_{i1}G_{i1}\right)x_{i1} + B_{i1}H_{i1}x_{ref\,1DQ} + C_{i1}v_{pDQ} \tag{25}$$

$$\dot{x}_{i2} = \left(A_{i2} + B_{i2}G_{i2}\right)x_{i2} + B_{i2}H_{i2}x_{ref\,2DQ} + C_{i2}v_{pDQ} \tag{26}$$

Furthermore, the load current in D-Q component is given as

$$\frac{d}{dt}\begin{bmatrix} i_{LD} \\ i_{LQ} \end{bmatrix} = \begin{bmatrix} -R_L/L_L & \omega \\ -\omega & -R_L/L_L \end{bmatrix}\begin{bmatrix} i_{LD} \\ i_{LQ} \end{bmatrix} + \begin{bmatrix} 1/L_L & 0 \\ 0 & 1/L_L \end{bmatrix}\begin{bmatrix} v_{pD} \\ v_{PQ} \end{bmatrix} \tag{27}$$

Therefore defining a composite state vector as

$$x_t^T = \begin{bmatrix} x_{i1}^T & x_{i2}^T & i_{LD} & i_{LQ} \end{bmatrix}$$

we can combine (25)-(27) to form the overall state space equation of the system.

Example 3: Let us consider the system shown in Fig. 6. Both the VSCs have the same parameters and the PCC voltage the same as discussed in Examples 1 and 2. The load resistance is 48.2 Ω and the inductance is 0.3 H. At the beginning, the following are assumed

$$V_{c1ref} = \left|\frac{11}{\sqrt{3}}\right| \angle 30° \text{ kV and } V_{c2ref} = \left|\frac{11}{\sqrt{3}}\right| \angle 20° \text{ kV}$$

This implies that P_{1ref} and Q_{1ref} are the same as those given in Example 2, while P_{2ref} = 526.9 kW and Q_{2ref} = 92.9 kVAr. With the system operating in steady state with these values, the reference for VSC-2 is suddenly changed at 0.05 s. The peak of the voltage is reduced to 95% of the nominal value, while its phase angle is changed to 30°. The reference powers are P_{2ref} = 731.79 kW and Q_{2ref} = 122.9 kVAr. The system responses for VSC-2 are shown in Figs. 7 and 8, where the solid lines depict the MATLAB results and the dotted lines depict the PSCAD outputs. In Fig. 7, the converter output voltages (v_{c2}) are shown. It can be seen that the PSCAD results are almost identical to those of MATLAB. The injected currents (i_{f2}) are shown in Fig. 8. It can be seen that the difference between the PSCAD simulation results and the predicted behaviors using MATLAB are very small and they match exactly in the steady state.

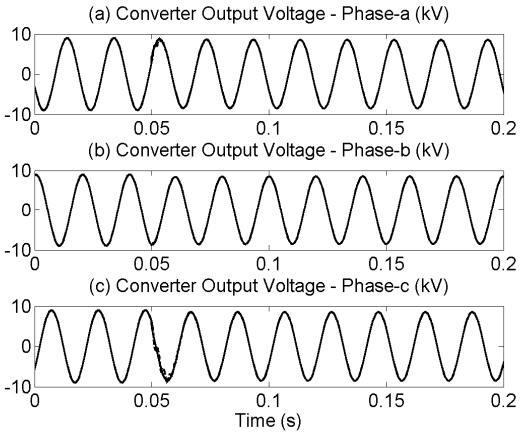

Figure 7. Simulated and predicted output voltages of VSC-2.

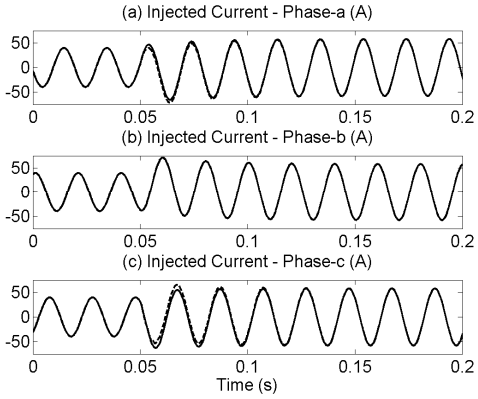

Figure 8. Simulated and predicted injected current by VSC-2.

V. MATHEMATICAL MODEL FOR AUTONOMOUS OPERATION

For this case, we assume that the PCC is a floating source, i.e., the voltage source v_p in Fig. 6 is absent and the two converters operate in parallel to share the load through droop characteristics. In this paper, we use an angle droop based on the active power [6] and a voltage magnitude droop based on reactive power. These are given by

$$\begin{aligned} \delta &= \delta_{rated} - m \times (P - P_{rated}) \\ V_{cm} &= V_{cm-rated} - n \times (Q - Q_{rated}) \end{aligned} \tag{28}$$

where $V_{cm\text{-}rated}$ and δ_{rated} are the rated voltage magnitude and angle respectively of a VSC when it is supplying the load to its rated power levels of P_{rated} and Q_{rated}.

Calculating real and power from instantaneous measurements can often lead to ripple in these quantities that will cause ripple in the converter references. To avoid this, the real and reactive power are passed through low pass filters before they are used in the droop equations. These low pass filters are given by

$$\begin{aligned} P_e &= \frac{\omega_c}{s + \omega_c} P \\ Q_e &= \frac{\omega_c}{s + \omega_c} Q \end{aligned} \tag{29}$$

where P and Q are instantaneous measured values and P_e and Q_e are their respective filtered outputs. We now substitute these values and δ and V_{cm} in (18), (19) and (22)

Since the PCC is not connected to an infinite bus, we have to eliminate the vector v_{pDQ} from the state equation. From (27), we can write

$$\begin{bmatrix} v_{pD} \\ v_{PQ} \end{bmatrix} = L_L \frac{d}{dt} \begin{bmatrix} i_{LD} \\ i_{LQ} \end{bmatrix} - L_L \begin{bmatrix} -R_L/L_L & \omega \\ -\omega & -R_L/L_L \end{bmatrix} \begin{bmatrix} i_{LD} \\ i_{LQ} \end{bmatrix} \tag{30}$$

Again, using Kirchoff's current law (KCL) at PCC, we get

$$i_{LD} = i_{f1D} + i_{f2D} \text{ and } i_{LQ} = i_{f1Q} + i_{f2Q} \tag{31}$$

Let us now define a new set of state vectors that contain only the state equations of the two converters. This is given by

$$x_c^T = \begin{bmatrix} x_{i1}^T & x_{i2}^T \end{bmatrix}$$

We can then express (30) in terms of the above state vector and its derivative as

$$\begin{bmatrix} v_{pD} \\ v_{PQ} \end{bmatrix} = A_P \dot{x}_c + B_P x_c$$

where the matrices A_p and B_p both have dimensions (12×2) and are computed from (30) and (31). From (24) and (32), we get the state space for the autonomous operation of the two VSCs as

$$\begin{aligned} \dot{x}_c = &\begin{bmatrix} A_{i1} + B_{i1}G_{i1} & \\ & A_{i2} + B_{i2}G_{i2} \end{bmatrix} x_c \\ &+ \begin{bmatrix} B_{i1}H_{i1} & \\ & B_{i2}H_{i2} \end{bmatrix} x_{crefDQ} + \begin{bmatrix} C_{i1} \\ C_{i2} \end{bmatrix} \left(A_P \dot{x}_c + B_P x_c \right) \end{aligned} \tag{33}$$

The above equation can be regrouped to form the state space equations for the autonomous operation of the VSCs as

$$\dot{x}_c = A_c x_c + B_c x_{crefDQ} \tag{34}$$

where

$$E = I_{12} - \begin{bmatrix} C_{i1} \\ C_{i2} \end{bmatrix} A_P$$

$$A_c = E^{-1} \left(\begin{bmatrix} A_{i1} + B_{i1}G_{i1} & \\ & A_{i2} + B_{i2}G_{i2} \end{bmatrix} + \begin{bmatrix} C_{i1} \\ C_{i2} \end{bmatrix} B_P \right)$$

$$B_c = E^{-1} \begin{bmatrix} B_{i1}H_{i1} & \\ & B_{i2}H_{i2} \end{bmatrix}$$

and I_{12} is a (12×12) identity matrix.

Example 4: Let us consider the same system discussed in Example 3, except the voltage source v_{ps}, which is removed. Also the filter inductance of VSC-2 has been changed to 0.3125 H. The droop coefficients from (28) are chosen as

$m_1 = 0.1$ rad/MW and $m_2 = 0.125$ rad/MW

$n_1 = 0.01$ kV/MVAr and $n_2 = 0.0125$ kV/MVAr

The cutoff frequency for the low pass filters are chosen as ω_c = 31.4 rad/s. The results are shown in Figs. 9 to 12. In all these figures, the MATLAB model and PSCAD simulation results are shown in sub-figures (a) and (b) and the errors between them are shown in (c). Fig. 9, the output voltage for phase-a of VSC-2 is shown. It can be seen that the maximum error between the MATLAB prediction and PSCAD simulation are less than 30 V, while the peak of the phase voltage is nearly 9 kV. This implies that the error is less than 0.33%. Similarly From the converter output (injected) current of VSC-2, shown in Fig. 10, it can be seen that the error is less than 0.2 A (0.4%). The output powers of the two converters are shown in Fig. 11. The errors are less than 0.5%. Similarly, from the reactive power plot shown in Fig. 12, it can be seen that the errors are less than 0.1 %. We can then surmise that the prediction model can predict the system behavior fairly accurately.

 ISBN: 978-1-61208-136-6

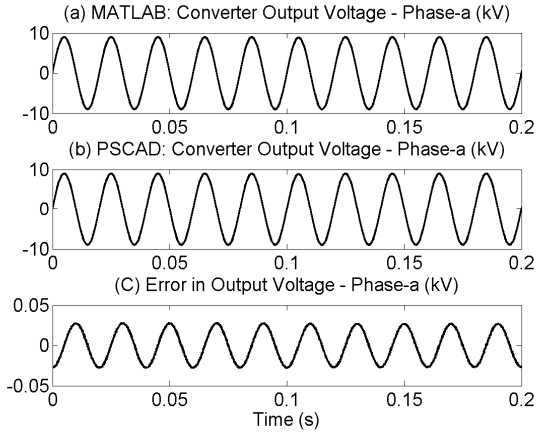

Figure 9. VSC-2 output voltage of phase-a and its error.

VI. SMALL SIGNAL MODEL FOR EIGEN ANALYSIS

Since the system response obtained by the mathematical model closely matches that of the PSCAD simulation, the VSC model developed in the previous sections can be used to find an autonomous small signal model of the system discussed in the previous section. To facilitate this, we must eliminate the reference vector (34).

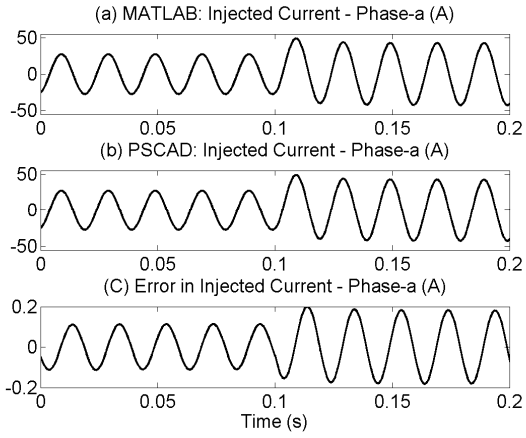

Figure 10. VSC-2 output current of phase-a and its error.

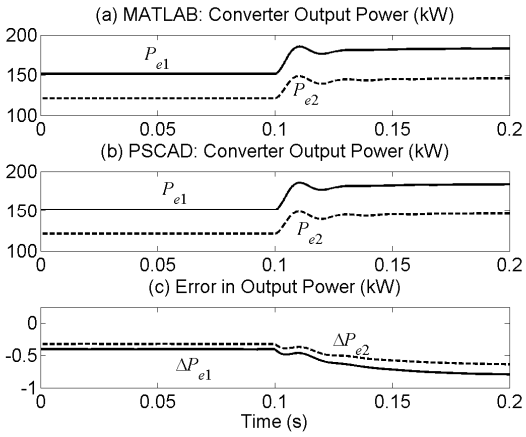

Figure 11. Output active power of the converters and their error.

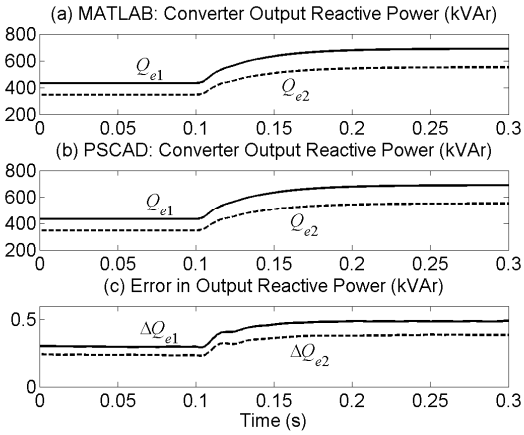

Figure 12. Output reactive power of the converters and their error.

From (29), (20) and (21), we can write

$$\dot{P}_e = -\omega_c P_e + \frac{3\omega_c}{2}\left(v_{cd} i_{fd} + v_{cq} i_{fq}\right)$$
$$\dot{Q}_e = -\omega_c Q_e + \frac{3\omega_c}{2}\left(v_{cq} i_{fd} - v_{cd} i_{fq}\right) \quad (35)$$

Linearizing the above equations around an operating point, we obtain

$$\Delta\dot{P}_e = -\omega_c \Delta P_e + \frac{3\omega_c}{2}\left(v_{cd0}\Delta i_{fd} + i_{fd0}\Delta v_{cd} + v_{cq0}\Delta i_{fq} + i_{fq0}\Delta v_{cq}\right)$$
$$\Delta\dot{Q}_e = -\omega_c \Delta Q_e + \frac{3\omega_c}{2}\left(v_{cq0}\Delta i_{fd} + i_{fd0}\Delta v_{cq} - v_{cd0}\Delta i_{fq} - i_{fq0}\Delta v_{dq}\right) \quad (36)$$

where the suffix Δ defines a perturbed quantity and subscript 0 signifies the nominal values. Defining a vector of active and reactive powers as

$$x_{pq} = \begin{bmatrix} P_{e1} & Q_{e1} & P_{e2} & Q_{e2} \end{bmatrix}^T$$

equation (26) can be written as

$$\Delta\dot{x}_{pq} = A_{pq}\Delta x_{pq} + B_{pq}\Delta x_c \quad (37)$$

where A_{pq} = diag($-\omega_c$ $-\omega_c$ $-\omega_c$ $-\omega_c$) and B_{pq} can be derived from (36).

We shall now replace the reference quantities by ΔP_e and ΔQ_e. To do that, we first linearize the droop equations (28) to obtain

$$\Delta\delta = -m \times \Delta P_e$$
$$\Delta V_{cm} = -n \times \Delta Q_e \quad (38)$$

Then from (18) and (23) we get

$$\begin{bmatrix} v_{cDref} \\ v_{cQref} \end{bmatrix} = \begin{bmatrix} \cos\delta & -\sin\delta \\ \sin\delta & \cos\delta \end{bmatrix} \begin{bmatrix} 0 \\ -V_{cm} \end{bmatrix}$$

Linearizing the above equation and substituting (38), we get

$$\begin{bmatrix} \Delta v_{cDref} \\ \Delta v_{cQref} \end{bmatrix} = \begin{bmatrix} -mV_{cmo}\cos\delta_0 & -n\sin\delta_0 \\ -mV_{cm0}\sin\delta_0 & n\cos\delta_0 \end{bmatrix} \begin{bmatrix} \Delta P_e \\ \Delta Q_e \end{bmatrix} \quad (39)$$

In a similar way, we find the references for the capacitor current are given as

$$\begin{bmatrix} \Delta i_{cDref} \\ \Delta i_{cQref} \end{bmatrix} = \begin{bmatrix} \lambda_1\sin\delta_0 & -\lambda_2\cos\delta_0 \\ -\lambda_1\cos\delta_0 & -\lambda_2\sin\delta_0 \end{bmatrix} \begin{bmatrix} \Delta P_e \\ \Delta Q_e \end{bmatrix} \quad (40)$$

where $\lambda_1 = m\omega C_f V_{cm0}$ and $\lambda_2 = n\omega C_f$. Finally replacing P_{ref} and Q_{ref} by P_e and Q_e respectively in (22), we get the linearized expressions for the injected currents as

$$\begin{bmatrix} \Delta i_{fDref} \\ \Delta i_{fQref} \end{bmatrix} = \frac{1}{V_{cm0}} \begin{bmatrix} \beta_{11} & \beta_{12} \\ \beta_{21} & \beta_{22} \end{bmatrix} \begin{bmatrix} \Delta P_e \\ \Delta Q_e \end{bmatrix} \quad (41)$$

where

$$\beta_{11} = -(2/3)(mQ_{e0}\sin\delta_0 + mP_{e0}\cos\delta_0 - \sin\delta_0)$$
$$\beta_{12} = -(2/3)\cos\delta_0 + ni_{fD0}$$
$$\beta_{21} = -(2/3)(mP_{e0}\sin\delta_0 + \cos\delta_0 - mQ_{e0}\cos\delta_0)$$
$$\beta_{22} = -(2/3)\sin\delta_0 + ni_{fQ0}$$

We can then write the reference vector in (34) as

$$\Delta x_{crefDQ} = M_c \Delta x_{pq} \quad (42)$$

where the elements of M_c are obtained from (39)-(41). Combing (34), (37) and (42), we get a homogeneous state space description of the complete system as

$$\begin{bmatrix} \Delta\dot{x}_c \\ \Delta\dot{x}_{pq} \end{bmatrix} = \begin{bmatrix} A_c & B_c M_c \\ B_{pq} & A_{pq} \end{bmatrix} \begin{bmatrix} \Delta x_c \\ \Delta x_{pq} \end{bmatrix} \quad (43)$$

This homogenous model can now be used for eigenvalue analysis.

Example 5: Let us consider the system discussed in Example 4. For eigenvalue analysis we vary a parameter m from 0.01×10^{-6} rad/W to 1.8×10^{-6} rad/W. Furthermore we choose the angle droop gains as $m_1 = m$ and $m_2 = 1.25\times m$. The plots of the dominant eigenvalues are shown in Fig. 13. It can be seen that for $m = 1.4785\times10^{-6}$ rad/W, the dominant eigenvalues cross the imaginary axis. Also the oscillation frequency of the dominant eigenvalues is roughly 314 rad/s (50 Hz). From eigenvectors it has been determined that these eigenvalues are associated with real and reactive power supplied by the VSCs.

To validate the eigenvalue results, PSCAD simulations studies are carried out for the same system. With the system operating at steady state with the nominal values of droop gains given in example, the value of m is changed suddenly at 0.1 s. Fig. 14 shows the plots of the real power output of VSC-2 for three different values of m. Fig. 14 (a) shows a damped oscillation for $m = 1.3\times10^{-6}$ rad/W, for which all the eigenvalues are not the left half s-plane. Fig. 14 (b) shows sustained oscillation for $m = 1.4785\times10^{-6}$ rad/W, for which the dominant eigenvalues are on the imaginary axis. The unstable case for which the dominant eigenvalues are on the right half s-plane are shown in Fig. 14 (c) for $m = 1.8\times10^{-6}$ rad/W. Also notice that there are five peaks and five troughs in each 0.1 s, indicating that the oscillation frequency is 50 Hz. This fundamental frequency oscillation is also predicted by the eigenvalues.

It is to be noted that n_1 and n_2 do not have a significant influence on the eigenvalues. However, if they are chosen arbitrarily large, the voltage regulation will fail and the converter output voltage will collapse leading to an instability in which no power can be transferred.

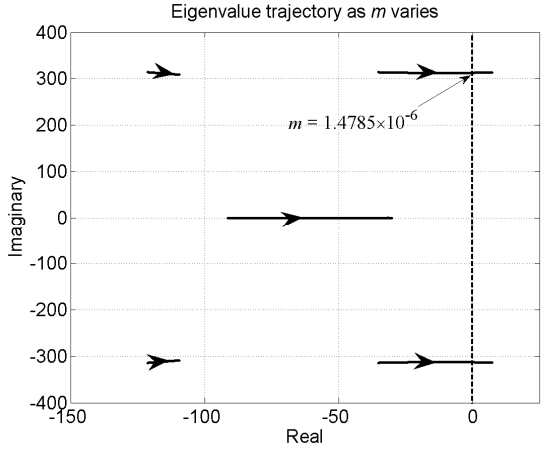

Figure 13. Eigenvalues plots from stability analysis.

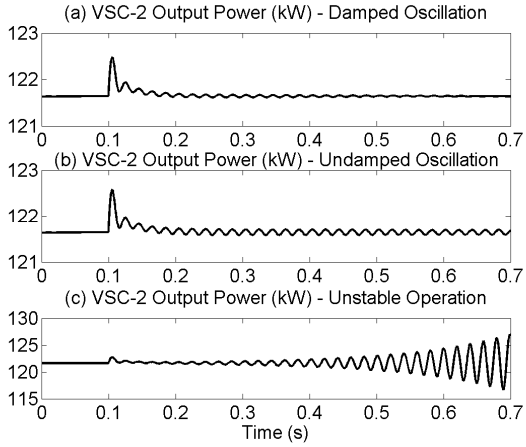

Figure 14. VSC-2 output power showing stable, undamped and unstable

VII. CONCLUSIONS

This paper proposes a method for developing a model for multiple VSCs operating in parallel in an autonomous mode. Each VSC is equipped with a T-filter and is assumed to operating in a full state feedback control of output voltage and current. The feedback gains are derived using LQR equations. Eigen value analysis and simulation studies are carried out in parallel. It has been shown that the system response predicted by the mathematical model matches the simulation results accurately, especially along the sliding line. Therefore the proposed model, with minor modification to include network, can be used for studying large systems when multiple converters operating in parallel to share loads.

ACKNOWLEDGMENT

The authors thank ABB Corporate Research, Sweden and Queensland University of Technology, Australia.

REFERENCES

[1] M. Reza, D. Sudarmadi, F. A. Viawan, W. L. Kling, and L. Van Der Sluis, "Dynamic Stability of Power Systems with Power Electronic Interfaced DG," Power Systems Conference and Exposition, PSCE'06, pp. 1423-1428, 2006.

[2] G. Ledwich and A. Ghosh. "Flexible DSTATCOM operating in voltage or current control mode," Generation, Transmission and Distribution, IEE Proceedings-Vol. 149, No. 2, pp. 215-224, 2002.

[3] J. Thunes, R. Kerkman, D. Schlegel, and T. Rowan, "Current regulator instabilities on parallel voltage-source inverters," IEEE Trans. Industry Applications, Vol. 35, No. 1, pp. 70-77, 1999.

[4] M. C. Chandorkar, D. M. Divan, and R. Adapa, "Control of parallel connected inverters in standalone ac supply systems," IEEE Trans. Industry Applications, Vol. 29, No. 1, pp. 136-143, 1993.

[5] J. M. Guerrero, L. G. de Vicuna, J. Matas, M. Castilla, and J. Miret, "A wireless controller to enhance dynamic performance of parallel inverters in distributed generation systems," IEEE Trans. Power Electronics, Vol. 19, No. 5, pp. 1205-1213, 2004.

[6] R. Majumder, A. Ghosh, G. Ledwich, and F. Zare, "Load sharing and power quality enhanced operation of a distributed microgrid," Accepted to appear in IET Renewable Power Generation, Vol. 3 , No. 2, pp. 109-119, 2008

[7] J. G. Slootweg and W. L. Kling, "Impacts of distributed generation on power system transient stability," Power Engineering Society Summer Meeting, 2002 IEEE Vol. 2, No. , pp. 862-867, 2002.

[8] M. N. Marwali, M. Dai, and A. Keyhani, "Stability Analysis of Load Sharing Control for Distributed Generation Systems," IEEE Trans. Energy Conversion, Vol. 22, No. 3, pp. 737-745, 2007.

[9] T. Suntio, M. Hankaniemi, and M. Karppanen, "Analysing the dynamics of regulated converters," Proc. IEE Electric Power Applications, Vol. 153, No. 6, pp. 905-910, 2006

[10] W. Li and L. Tsung-Jen, "Stability and Performance of an Autonomous Hybrid Wind-PV-Battery System," International Conference on Intelligent Systems Applications to Power Systems, pp. 1-6, 2007.

[11] A. Ghosh and A. Joshi, "A new approach to load balancing and power factor correction in power distribution system," IEEE Trans. Power Delivery, Vol. 15, No. 1, pp. 417-422, 2000.

[12] B. D. O. Anderson and J. B. Moore, Linear Optimal Control, Prentice-Hall, Englewood Cliffs, N.J., 1971.

[13] J. J. E. Slotine and W. Li, Applied Nonlinear Control, Prentice-hall, Englewood Cliffs, N.J., 1991.

[14] H. K. Khalil, Nonlinear Systems, 3rd Ed., Prentice-Hall, Upper Saddle River, N.J., 2002.

 ISBN: 978-1-61208-136-6